



HAL
open science

Mapping out the electron-electron interaction in gas phase C60

Jamal Berakdar, Oleg Kidun

► **To cite this version:**

Jamal Berakdar, Oleg Kidun. Mapping out the electron-electron interaction in gas phase C60. Philosophical Magazine, 2006, 86 (17-18), pp.2529-2536. 10.1080/14786430500333307 . hal-00513616

HAL Id: hal-00513616

<https://hal.science/hal-00513616>

Submitted on 1 Sep 2010

HAL is a multi-disciplinary open access archive for the deposit and dissemination of scientific research documents, whether they are published or not. The documents may come from teaching and research institutions in France or abroad, or from public or private research centers.

L'archive ouverte pluridisciplinaire **HAL**, est destinée au dépôt et à la diffusion de documents scientifiques de niveau recherche, publiés ou non, émanant des établissements d'enseignement et de recherche français ou étrangers, des laboratoires publics ou privés.



**Mapping out the electron-electron interaction in gas phase
C60**

| | |
|-------------------------------|--|
| Journal: | <i>Philosophical Magazine & Philosophical Magazine Letters</i> |
| Manuscript ID: | TPHM-05-Jan-0013.R1 |
| Journal Selection: | Philosophical Magazine |
| Date Submitted by the Author: | 02-May-2005 |
| Complete List of Authors: | Berakdar, Jamal; Max-Planck Institute of Microstructure Physics, Theory Kidun, Oleg; Max-Planck Institute of Microstructure Physics, Theory |
| Keywords: | electronic spectroscopy, electronic spectra |
| Keywords (user supplied): | electronic correlation, electron coincidence spectroscopy, electron energy loss spectroscopy |
| | |



Submitted to *Phil. Mag.*

Mapping out the electron-electron interaction in gas phase C₆₀

O. Kidun and J. Berakdar^a

Max-Planck-Institute of Microstructure Physics, Weinberg 2, 06120 Halle, Germany

Abstract— In this work we present a theory for studying the details of the screened electron-electron interaction in fullerenes by means of the coincident electron emission upon charged particle impact. The cross sections for this process are expressed in terms of the screened electron-electron interaction and evaluated within the random phase approximation. We performed full quantum mechanical calculations for the cross sections and obtained a fair agreement with available experiments. Furthermore, we present theoretical angular and energy-resolved cross sections to underline the wealth of information that can be gained by future experiments.

^a) Corresponding author, e-mail: jber@mpi-halle.mpg.de

§1. INTRODUCTION

A variety of physical properties of electronic materials are governed by the cooperative behaviour of the electrons. Prominent examples are the emergence of Wannier excitons in wide band semiconductors. In narrow band materials, e.g. in 3d transition metal oxides or in rare earths, Coulomb interactions may result in insulating (magnetic) ground states. The role of electronic correlation is ubiquitous in that it also determines some important features of molecular and polymeric materials. For example C_{60} doped with alkali metals acquires superconductive features, hence calling for an investigations of the role of the electron-electron (e-e) interaction in this molecular material [1,2]: A theoretical study of the nature of the e-e interaction in solid (ordered) phase C_{60} concluded that the screened on-site molecular Coulomb integral is ~ 2.1 eV [3]. In addition to this energetic feature, an important concept for inspecting the e-e interaction is screening. Screening effects can be quantified by the dielectric function [4]. Experiments reported in [5] give an estimate of 4.6 for the value of C_{60} macroscopic dielectric function whereas Ref.[6] estimates this value to be 3.6. These numbers mean a weak screening in *solid* C_{60} ; however, they do not offer an insight into the angular and the energy dependence of screening of the e-e interaction, in particular as far as gas phase fullerenes are concerned. It is the purpose of this work to present a new spectroscopic tool to shed light on the various facets of the electron-electron interaction in matter. The method relies on disturbing the system by charged particles. The system may then react by ejecting one or more electrons. As shown below, resolving the energies and momenta of the final-state particles offers a possibility to access information on the details of the electron-electron interaction.

The paper is organized as follows. In section 2 we present a general framework for the treatment of screening in collision processes. In section 3 the theory is applied electron and proton scattering from fullerenes C_{60} . Section 4 contains conclusions and final remarks. Unless otherwise specified atomic units (a.u.) $\hbar=e=m_e=1$ are used throughout.

§2. GENERAL CONSIDERATION

A schematic view of the process under study is depicted in Fig. 1. A target prepared in the quantum state $|\phi_v\rangle$ is perturbed by a projectile that has a specified quantum state $|\mathbf{k}_0\rangle$, where \mathbf{k}_0 is the momentum of the impinging particle. In the final state two electrons emerge with the asymptotic momenta \mathbf{k}_1 and \mathbf{k}_2 . In electron energy loss spectroscopy, EELS, only one electron [7] is measured. One usually assumes that this electron is the projectile electron that has suffered some amount of

energy and momentum loss. As well-established, the EELS cross section is then related to the imaginary part of the dielectric function. The difference between EELS and the process shown in Fig.1 is inferred from the energy balance: If the energy lost by the projectile is not sufficient to overcome the work function the electron emission channel is closed, i.e. the process in Fig.1 is not possible. In contrast in this case one does measure an EELS signal associated with neutral excitations such as plasmon generation. On the other hand the energy loss of the projectile may well be as high as to excite a target electronic state into the vacuum. In such a case the process in Fig.1 contributes to the EELS cross section. However, what is then measured in EELS provides only integral information. More details are obtained by detecting both excited states \mathbf{k}_1 and \mathbf{k}_2 at the same time. Another possibility to trace the occurrence of the process in Fig.1 is to detect the charge state of the target in the final channel. This possibility allows measuring for example the integrated (total) cross sections while still singling out the electron emission channel.

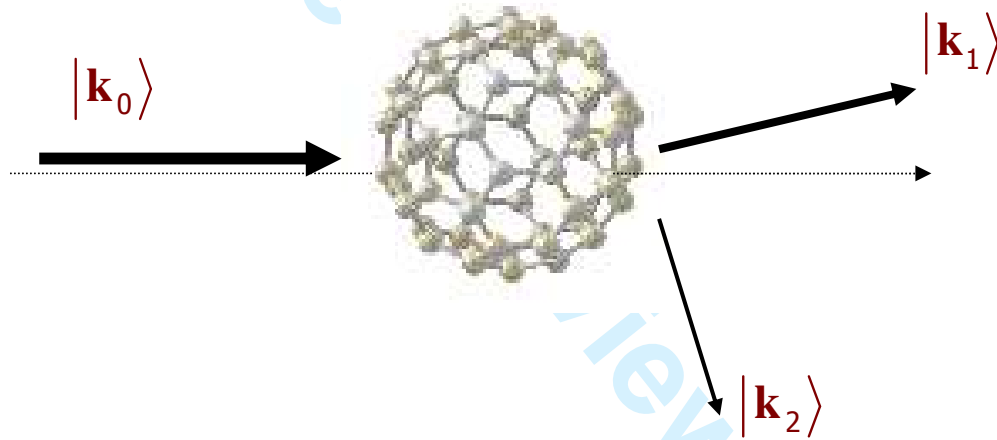


Figure 1: A schematic drawing of the emission process of an electron with a wave vector \mathbf{k}_2 for C_{60} upon the impact of a charged particle with the wave vector \mathbf{k}_0 . The momentum of the scattered particle is \mathbf{k}_1 . The z axis is chosen as the direction of the incoming particle \mathbf{k}_0 .

The transition matrix elements $T(\mathbf{k}_1\mathbf{k}_2, \phi, \mathbf{k}_0)$ of the electron emission process (Fig.1) can be evaluated in first-order perturbation theory in the (unknown) electron-electron interaction U_{eff} , which amounts to using the so-called random-phase approximation, RPA (in the case of a projectile electron one has also to account for exchange effects, in such a case we use RPAE, i.e. RPA with exchange). A posteriori we will find that this approach is justified for moderately large systems, such C_{60} , due to the fact that screening is substantial. Within RPAE the matrix elements $T(\mathbf{k}_1\mathbf{k}_2, \phi, \mathbf{k}_0)$ are given by the equation [8]

$$\begin{aligned}
T(\mathbf{k}_1 \mathbf{k}_2, \phi_\nu \mathbf{k}_0) &= \langle \mathbf{k}_1 \mathbf{k}_2 | U_{eff} | \phi_\nu \mathbf{k}_0 \rangle = \\
\langle \mathbf{k}_1 \mathbf{k}_2 | U | \phi_\nu \mathbf{k}_0 \rangle &+ \sum_{\substack{\varepsilon_h > \mu \\ \varepsilon_p \leq \mu}} \left(\frac{\langle \phi_p \mathbf{k}_2 | U_{eff} | \phi_\nu \phi_h \rangle \langle \phi_h \mathbf{k}_1 | U | \mathbf{k}_0 \phi_p \rangle}{\varepsilon_0 - (\varepsilon_p - \varepsilon_h - i\delta)} - \frac{\langle \phi_h \mathbf{k}_2 | U_{eff} | \phi_\nu \phi_p \rangle \langle \phi_p \mathbf{k}_1 | U | \mathbf{k}_0 \phi_h \rangle}{\varepsilon_0 + (\varepsilon_p - \varepsilon_h - i\delta)} \right).
\end{aligned} \tag{1}$$

This integral equation has to be solved (numerically) in order to obtain the effective interaction U_{eff} between the test particle (the projectile) and the target electronic state ϕ_ν . In eq.(1) ε_0 is the energy of the incoming particle and $\varepsilon_{p/h}$ are the energies of respectively the particle and the hole states ϕ_p and ϕ_h and U is the naked Coulomb interaction. The sum in eq. (1) runs over all particle and hole states up to the Fermi level μ . To make more clearly the connection between equation (1) and the linear response theory we write eq. (1) formally as $U_{eff} = U + U_{eff} \Pi U$ where Π is the polarization propagator. This relation can be rewritten as $U_{eff} = U / \varepsilon$, where $\varepsilon = 1 - \Pi U$ is the dielectric function.

Currently only integrated cross sections for the process of Fig.1 have been measured [9,10], i.e. these experiments do not resolve the momenta and the spins $\sigma_{1,2}$ of the particles in the final state, but they do resolve the projectile energy and the target charge states. To compare with these experiments we have to evaluate the total cross section W as

$$W(\varepsilon_0) = \frac{(2\pi)^2}{k_0} \int d^3 \mathbf{k}_1 d^3 \mathbf{k}_2 \sum_{\sigma_1 \sigma_2 \phi_\nu} \left| \langle \mathbf{k}_{1,\sigma_1} \mathbf{k}_{2,\sigma_2} | U_{eff} | \phi_\nu \mathbf{k}_0 \rangle \right|^2. \tag{2}$$

From eqs.(1,2) it is clear that the calculations of the matrix elements and the cross sections entail the knowledge of the electronic particle and hole states of the target in the ground state (before the collision) as well as its scattering states. These states have to be calculated independently for each individual system and with this knowledge we then solve for the integral equation (1) to determine the dressed particle-particle interaction U_{eff} . So, even though U has a universal structure independent of the system, U_{eff} is in general strongly system dependent. It is this dependency which can be revealed by the process depicted in Fig.1.

§3. NUMERICAL RESULTS

As an example we calculate the total cross section (2) for the ionization of the valence band electrons in C_{60} by numerically solving for eq.(1) and then performing a numerical Monte Carlo integration to evaluate the six dimensional integral in eq.(2).

The single hole and particle states of the fullerene are derived from self-consistent Hartree-Fock calculations; thus we incorporate (for the ground state calculations) the mean-field part of the electron-electron interactions and exact exchange effects. Both bound and scattering wave functions are calculated simultaneously using the non-local variable phase method [11-13] which proved indispensable for the numerical realization. For the fullerene shell we employ a model potential that incorporates correctly the experimentally determined radius of C_{60} , the distance between the neighboring carbon nuclei (C-C bond length) and the affinity energy of the electron to the singly charged fullerene. This model was used previously in Refs.[14,15], however the calculation were made on the basis of density functional theory within the local-density approximation and without performing the RPAE loop. The resulting potential, formed by the carbon ions and the localized core electrons, is a shifted potential well: $V_{ion}(r) = V_0$ for $R - \delta < r < R$, and $V_{ion}(r) = 0$ elsewhere. Here $R \sim 6.65$ *a.u.* is the radius of the fullerene. The average C-C bond length is the thickness of the well $\delta \sim 2.69$ *a.u.*. The depth V_0 is determined such that the experimental value of the first ionization potential of C_{60} is 7.6 *eV* and the number of valence electrons is 240.

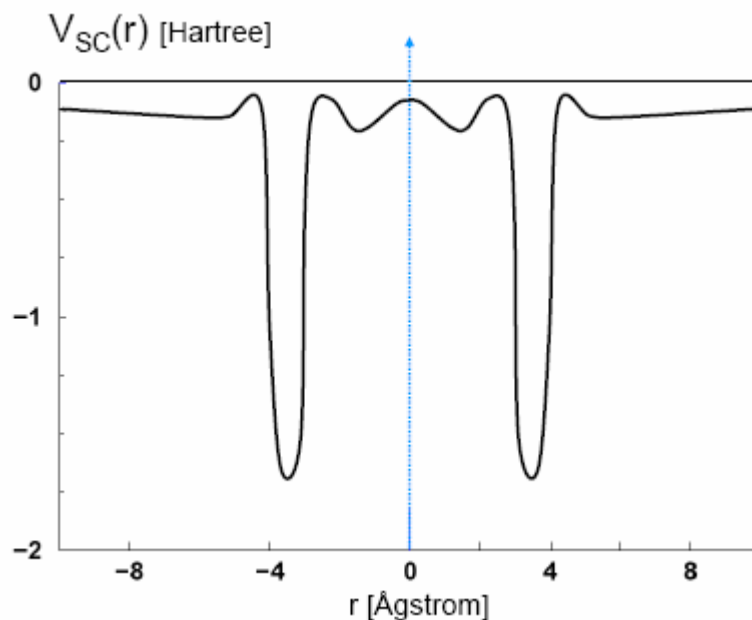


Fig.2 Calculated local part of the self-consistent single-particle potential $V_{SC}(r)$ for a valence band electron in C_{60} that has a vanishing angular momentum. V_{SC} is plotted as a function of the radial distance r measured from the cage center of C_{60} .

To illustrate the structure of the potential the valence electrons are experiencing we plot in Fig.2 the calculated local part only of the self-consistent single-particle potential V_{SC} for a valence band electron with a zero angular momentum. From this figure it is evident that the mean-field part of the electron-electron interaction and the local part of the exchange interaction result in a marked modification of the external potential V_{ion} (in fact the potential V_{SC} is non-local and contains in general a centrifugal term).

The numerical results obtained upon performing the calculations required by eq.(2) are shown in Fig.3 and compared to other calculations and available experiments. Two important observations can be made here: The effect of screening is substantial in the low frequency regime even for relatively small systems such as C_{60} . In the high frequency regime we see no effect of screening because the characteristic frequency of the retarded response of the target is far off the perturbation frequency.

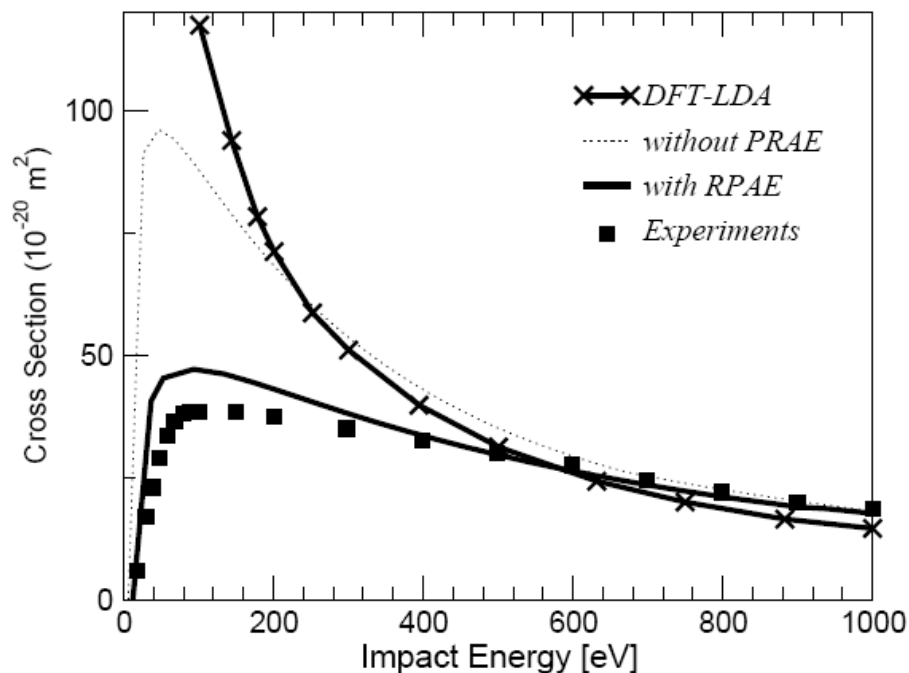


Figure 3: The absolute total cross section for the removal of one electron from C_{60} following the impact of an electron with the energy displayed on the axis. The experimental data (full squares) are due to Refs. [9, 10]. The solid curve with crosses is the result of density functional theory calculations done within local-density approximation and reported in Ref. [14]. The dotted curve shows the present theory without RPAE. Theoretical results based on RPAE are shown by the solid curve.

1
2
3
4
5
6
7
8
9
10
11
12
13
14
15
16
17
18
19
20
21
22
23
24
25
26
27
28
29
30
31
32
33
34
35
36
37
38
39
40
41
42
43
44
45
46
47
48
49
50
51
52
53
54
55
56
57
58
59
60

These two observations justify our use of the first-order perturbation theory in the projectile electron-valence electron interaction (in the high energy regime, this approach is valid anyway). Fig.3 evidences that electron emission is suppressed by the screening of the perturbation caused by the incoming particles. The delocalized valence electrons cooperatively rearrange as such as to reduce at the C₆₀ cage surface the external electric field. This is not achievable for high projectile energies and small impact parameter and hence screening has no sizable effect in the high energy range in Fig.3. This interpretation follows also from eq.(1): In the simplest approximation the cross section (2) is proportional to the form factor of $U_{eff}(q)$ where $\mathbf{q}=\mathbf{k}_0-\mathbf{k}_1$ is the momentum transfer vector. From the theory of the homogenous electron gas we know that in the long-wave length limit $U_{eff}(q) \sim U_{eff,TF}(q) \sim 1/(q^2 + \lambda^2)$ where $1/\lambda$ is the screening length. Our calculations show indeed that the Fourier transform of the potential U_{eff} can, to some extent, be modeled by the potential $U_{eff,TF}(q)$. On the other hand from the form of $U_{eff,TF}(q)$ we conclude that for a large q , i.e. close collision, $U_{eff,TF}(q) \rightarrow U(q)$ where $U(q)$ is the naked Coulomb interaction, but for a small momentum transfer, i.e. distant collisions, we infer that $U_{eff,TF}(q) \sim constant = 1/\lambda^2$, which indeed explains the saturation effect of the cross section observed in Fig.3 as compared to the unscreened calculations.

The calculations and the experiments shown in Fig.3 contain a contribution from exchange effects due to the fact that the projectile is an electron. To get an insight both experimentally and theoretically in the importance of these effects one can use a test projectile particle other than electrons. Here we employ protons. Neglecting screening we find within our first order theory for the projectile target interaction that there should be no difference in the ionization cross sections induced by equivelocity projectiles that have the same magnitude of charge, e.g. equal-velocity electrons and protons should lead to the same ionization cross section. Applying RPA a difference between these two cases arises solely due to the fact that in case of proton the exchange contributions are absent.

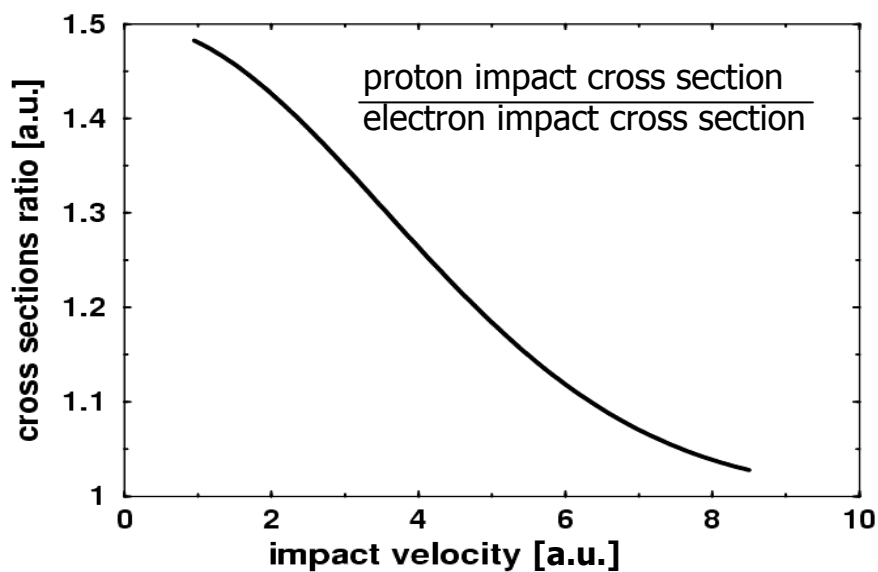


Figure 4: Ratio of absolute total ionization cross sections of the valence band of C₆₀ by proton and electron impact as a function of the projectile impact velocity. The electron impact ionization cross section is shown by the solid curve in Fig.3.

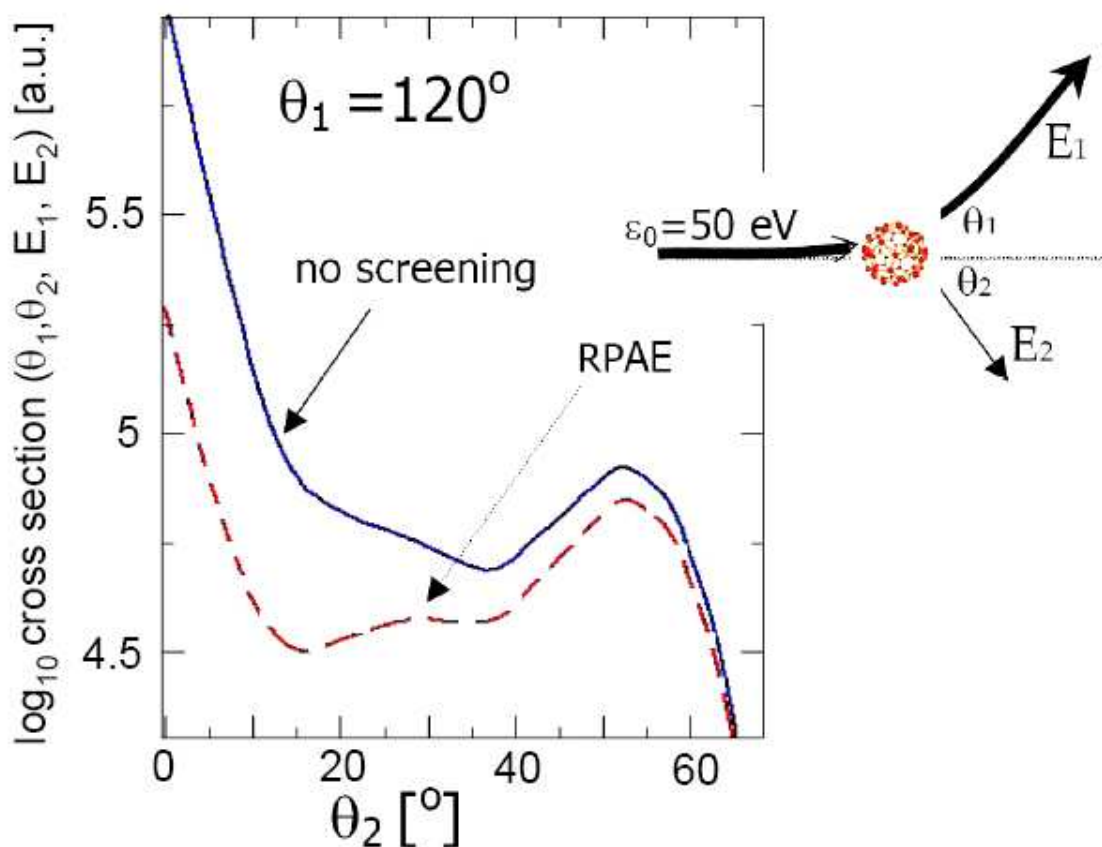


Figure 5: The angular dependence of the fully differential cross section for the emission of one electron from C₆₀ with 1 eV energy following the impact of 50 eV electrons. A schematic of the scattering geometry is depicted. The scattering angle θ_1 of the scattered electron is fixed at 120° whereas the emission angle θ_2 of the second electron is varied. Calculations with (dashed line) and without (solid line) screening are compared.

1
2
3
4
5
6
7
8
9
10 These contributions are quite sizable as demonstrated by Fig.4 where the ratio of the cross sections for
11 proton and electron impact ionization of the valence band of C_{60} is plotted against the impact velocity
12 of the projectile. At a velocity of approximately 10 a.u. screening effects become negligible and
13 protons and electrons are equivalently effective in ionizing the target, as also follows from the first
14 Born theory for ionization. At lower velocities however, exchange effects active in case of a projectile
15 electron suppress the ionization cross sections by a factor of up to 1.5, as compared to the proton-
16 impact ionization cross sections.
17

18
19 To exploit the full power of the present spectroscopic technique one should perform angular and
20 energy resolve coincidence measurements. Such experiments allow accessing experimentally the
21 energy and angular dependence of the magnitude $|T|^2$ of the transition matrix elements, as given by
22 eq.(1). As evident from eq.(1) $|T|^2$ in turn contains information on the energy and the angular
23 dependence of the screened particle-particle interaction characteristic for the system under study. This
24 kind of experiments has not been conducted yet. Typical calculations are shown in Fig.5. The origin
25 of the structures seen in the cross sections lies in the nature of U_{eff} and in the details of the electronic
26 structure of the target. In the context of the present work we emphasize the strong angular dependence
27 of the electron-electron screening; different values of θ_1 in Fig.5 yield different angular distributions
28 of the cross section as function of θ_2 . To the best of our knowledge such a detailed study of the
29 screened electron-electron interaction in electronic material is not accessible by any other
30 spectroscopic tool. In particular, EELS is not capable of providing such information.
31
32
33
34
35
36
37
38
39
40
41
42
43
44
45
46
47
48
49

50 §5. SUMMARY AND CONCLUSIONS

51 In summary, in this theoretical study we envisaged the use of coincident electron emission
52 from fullerene by charged particle impact as a tool for studying the details of the screened electron-
53 electron interaction. We presented a formal theory to evaluate the cross sections for this process and
54 performed full quantum calculations that are in fair agreement with available experiments.
55 Furthermore, we pointed out the need for further experimental investigations to separate the exchange-
56
57
58
59
60

1 driven contributions to screening and to obtain full information on the angular and energy dependence
2 of the screening of the electron-electron interaction in the valence band of fullerenes. As shown in Ref
3 [8] much of these findings are also valid for other nano-size systems such as metal clusters.
4
5
6
7
8
9
10
11
12
13
14

15 REFERENCES

- 16
17
18 [1] A. F. Hebard et al., Nature 350, 600 (1991).
19 [2] R.W. Lof et al., Phys. Rev. Lett. 68, 3924 (1992); J. Electron. Spectrosc. Relat. Phenom. 72, 83
20 (1995).
21 [3] D. P. Joubert, J. Phys.: Condens. Mat. **5**, 8047 (1993).
22 [4] O. Gunnarsson and G. Zwicknagel, Phys. Rev. Lett. **69**, 957 (1992).
23 [5] P. L. Hansen *et al.*, Chem. Phys. Lett. **181**, 367 (1991).
24 [6] S. R. Ren *et al.*, Appl. Phys. Lett. **59**, 2678 (1991).
25 [7] H. Ibach and DL Mills, *Electron Energy Loss Spectroscopy and Surface Vibrations*,
26 (Academic Press, New York, 1982.)
27 [8] O. Kidun, J. Berakdar, Phys. Rev. Lett. **87**, 263401 (2001).
28 [9] S. Matt *et al.*, J. Chem. Phys. **105**, 1880 (1996).
29 [10] V. Foltin *et al.*, Chem. Phys. Lett. **289**, 181 (1998).
30 [11] F. Calogero, Nuovo Cimento **33**, 352 (1964);
31 [12] V. Babikov, *Method of the phase functions in quantum mechanics* (Moskow, Nauka, 1971).
32 [13] O. Kidun, N. Fominykh, J. Berakdar, J. Phys. A, **35**, 9413 (2002).
33 [14] S. Keller, E. Engel, Chem. Phys. Lett. **299**, 165 (1999); S. Keller, Eur. Phys. J. D **13**, 51 (2001).
34 [15] M. Brack, Rev. Mod. Phys. **65**, 677 (1993).
35
36
37
38
39
40
41
42
43
44
45
46
47
48
49
50
51
52
53
54
55
56
57
58
59
60